# ORIGINAL RESEARCH

Complement-5 Inhibition Deters Progression of Fulminant Hepatitis to Acute Liver Failure in Murine Models

Jiro Kusakabe,[1] Koichiro Hata,[1,2] Hidetaka Miyauchi,[1] Tetsuya Tajima,[1] Yi Wang,[3] Ichiro Tamaki,[1] Junya Kawasoe,[1] Yusuke Okamura,[1] Xiangdong Zhao,[1] Tatsuya Okamoto,[1] Tatsuaki Tsuruyama,[4] and Shinji Uemoto[1,2]

[1]Division of Hepato-Biliary-Pancreatic Surgery and Transplantation, Department of Surgery, Kyoto University Graduate School of Medicine, Kyoto, Japan; [2]Organ Transplant Unit, Kyoto University Hospital, Kyoto, Japan; [3]Alexion Pharmaceuticals, New Haven, Connecticut; and [4]Center for Anatomical, Pathological, and Forensic Medical Research, Kyoto University Graduate School of Medicine, Kyoto, Japan
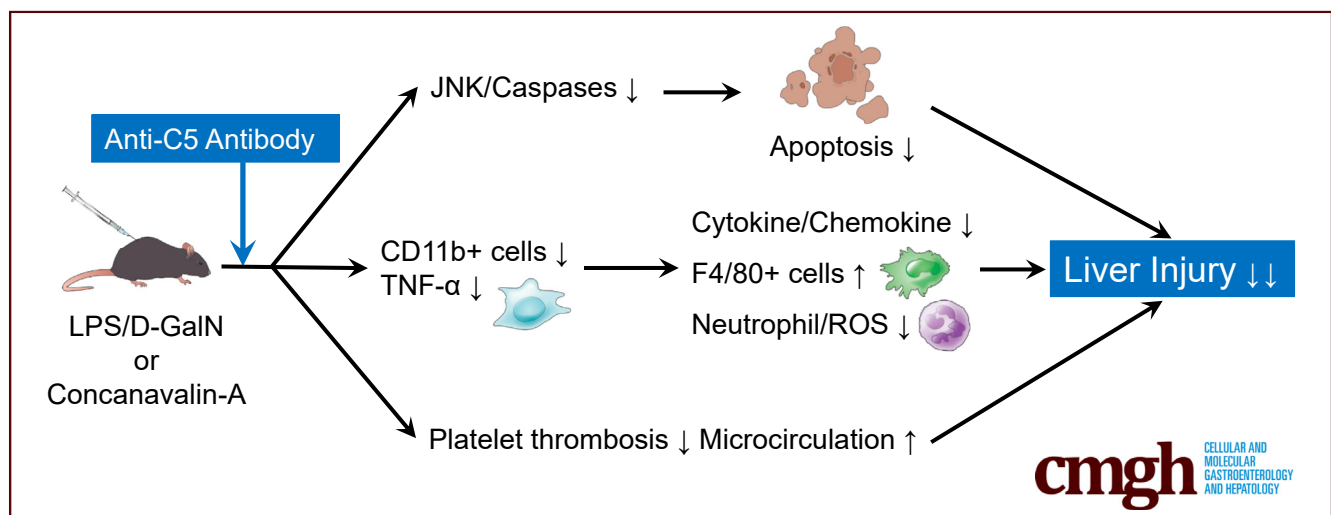
SUMMARY

Anti-C5-antibody (Ab), whose efficacy is superior to that of C5a blockade, exerts a marked therapeutic effect on different acute liver failure (ALF) mice models. Anti-C5-Ab potentially provides a novel promising strategy to inhibit the progression of acute hepatitis to ALF.

BACKGROUND & AIMS: Acute liver failure (ALF) is a life-threatening condition with limited treatment alternatives. ALF pathogenesis seemingly involves the complement system. However, no complement-targeted intervention has been clinically applied. In this study, we aimed to investigate the potential of Complement-5 (C5)-targeted ALF treatment.

METHODS: ALF was induced in C5-knockout (KO, B10D2/oSn) mice and their wild-type (WT) counterparts (B10D2/nSn) through intraperitoneal lipopolysaccharide (LPS) and D-galactosamine (D-GalN) administration. Thereafter, monoclonal anti-C5 antibody (Ab) or control immunoglobulin was administered intravenously. Furthermore, a selective C5a-receptor (C5aR) antagonist was administered to WT mice to compare its efficacy with that of anti-C5-Ab-mediated total C5 inhibition. We clarified the therapeutic effect of delayed anti-C5-Ab administration

after LPS/D-GalN challenge. We also assessed the efficacy of anti-C5-Ab in another ALF model, using concanavalin-A.

RESULTS: Liver injury was evident 6 hours after LPS/D-GalN administration. C5-KO and anti-C5-Ab treatment significantly improved overall animal survival and significantly reduced serum transaminase and high-mobility group box-1 release with decreased histological tissue damage. This improvement was characterized by significantly reduced CD41+ platelet aggregation, maintained F4/80+ cells, and less infiltration of CD11+/Ly6-G+ cells with lower cytokine/chemokine expression. Furthermore, C5-KO and anti-C5-Ab down-regulated tumor necrosis factor-α production by macrophages before inducing marked liver injury. Moreover, single-stranded-DNA cells and caspase activation were reduced, indicating significant attenuation of apoptosis. Anti-C5-Ab treatment protected the liver more effectively than the C5aR antagonist, and its delayed doses were hepatoprotective. In addition, anti-C5-Ab treatment was effective against concanavalin-A–induced ALF.

CONCLUSIONS: C5 inhibition effectively suppresses progression to ALF in mice models of fulminant hepatitis, serving as a new potential treatment strategy for ALF. (Cell Mol Gastroenterol Hepatol 2021;11:1351–1367; https://doi.org/10.1016/j.jcmgh.2021.01.001)

Acute liver failure (ALF) is a life-threatening patho-logical condition with various etiologies such as viral or autoimmune hepatitis, hepatotoxic compounds, and metabolic or genetic diseases[1] and is characterized by massive hepatocyte necrosis, rapid deterioration of liver function, encephalopathy or coma, and high mortality. Apart from the direct effects of hepatotoxic agents, various immune cells are activated and recruited to the liver, regardless of the etiology.[2] They produce numerous proinflammatory media-tors including cytokines, chemokines, proteases, and reactive oxygen or nitrogen species, inducing apoptotic or necrotic changes in hepatocytes.[3] Although the mechanisms under-lying these deleterious conditions are known, treatment al-ternatives remain limited. Moreover, liver transplantation, a rapid salvage procedure, is still required in approximately 30% of ALF patients.[4,5]

The complement system plays a key role in liver homeo-stasis and immune responses[6] and is involved in the patho-genesis of various diseases, including fibrosis, alcoholic disease, nonalcoholic steatohepatitis, hepatocellular carcinoma, and liver ischemia-reperfusion injury.[6–11] C3-knockout (KO), C3aR (C3a-receptor)/C5aR-antagonists, and CR2-fH (complement-receptor-2 and factor-H) protect the liver from lipopolysac-charide (LPS)/D-galactosamine hydrochloride (D-GalN)–induced injury in mice.[12] Moreover, the C5a-C5aR pathway is important in the pathogenesis of murine fulminant hepatitis via its induction of the expression of fibrinogen-like protein 2.[13,14] Thus, the complement system may be closely involved in ALF pathogenesis; however, complement-targeting interventions against ALF have yet to be applied in the clinical setting.

Paroxysmal nocturnal hemoglobinuria was the first complement-mediated disease for which Eculizumab, a hu-manized monoclonal antibody (mAb) to the terminal com-plement component-5 (C5) was approved.[15] Thereafter, its indications have expanded to various complement-mediated refractory diseases, including atypical hemolytic uremic syndrome, refractory generalized myasthenia gravis, and aquaporin-4 antibody–positive neuromyelitis optica spec-trum disorder.[16–19] Furthermore, eculizumab treatment reportedly alleviates intractable symptoms in severe Guil-lain-Barré syndrome.[18] It inhibits the enzymatic cleavage of C5 to C5a and C5b by directly interacting with C5. Without interfering with other host immune processes, eculizumab prevents not only C5a-mediated chemotaxis among proin-flammatory immune cells but also the assembly of C5b-9, known as the membrane attack complex (MAC), which triggers caspase activation through NLRP3 (Nod-like re-ceptor family protein 3) inflammasome activation.[20,21]

Therefore, we hypothesized that C5-targeted regulation is a promising early interventional strategy for ALF. In this study, we aimed to investigate the role of C5 in ALF path-ogenesis and the therapeutic potential of C5 regulators with anti-C5-Ab in ALF.

Results

Chronological Alterations in Complement Hemolytic Activity in ALF

To determine whether anti-C5-Ab treatment completely inhibited systemic terminal complement activity in our mouse model, serum hemolytic activity was assessed after 30 minutes and 1, 3, 7, 9, and 10 days of intravenous anti-C5-Ab administration. As shown in Figure 1*A*, 1 dose of BB5.1 completely inhibited complement hemolytic activity until day 9, and activity recovered on day 10.

Furthermore, hemolytic activity in the ALF model was assessed with or without anti-C5-Ab administration. As shown in Figure 1*B*, serum complement activity was grad-ually increased on LPS/D-GalN administration up to 203% at 4 hours in the control mice (*WT+Control-IgG*) and was completely inhibited upon anti-C5-Ab treatment throughout the study period.

As shown in Figure 1*C*, MAC deposition was observed in pericentral zone 3 after LPS/D-GalN administration in con-trol mice (*WT+Control-IgG*) but not in the other groups. These findings indicate that C5b-9 (MAC) directly targeted hepatocytes; this effect was completely suppressed by C5-KO and anti-C5-Ab treatment.

Transaminase Release and Histopathological Findings

In *WT+Control-IgG*, LPS/D-GalN–induced liver injury was detected at 4 hours, which became severe after 6 hours. Hepatocellular damage, reflected by serum alanine amino-transferase (ALT) levels, was significantly decreased by anti-C5-Ab treatment and C5-KO at 6 hours ($P < .001$) (Figure 1*D*). Histopathological grading revealed significantly alleviated liver damage in all treatment groups compared with that in *WT+Control-IgG* mice at 6 hours ($P < .001$) (Figure 1*E*). Representative tissue sections are shown in Figure 1*F*, revealing the alleviation of apoptosis and necrosis and inflammation after C5 inhibition (C5-KO and anti-C5-Ab) compared with that in *WT+Control-IgG* mice ($P < .001$).

High-Mobility Group Box-1 Release

High-mobility group box-1 (HMGB-1) is intricately involved in the progression of LPS/D-GalN–induced ALF[22] and is passively released from dying cells,[23] leading to massive release of proinflammatory cytokines and

chemokines by interacting with soluble molecules such as Toll-like receptor-4. Therefore, to comprehensively evaluate liver damage and its impact on subsequent inflammatory

responses, serum HMGB-1 concentrations were determined using enzyme-linked immunosorbent assay (ELISA). HMGB-1 was detected at 4 hours and its level sharply increased at
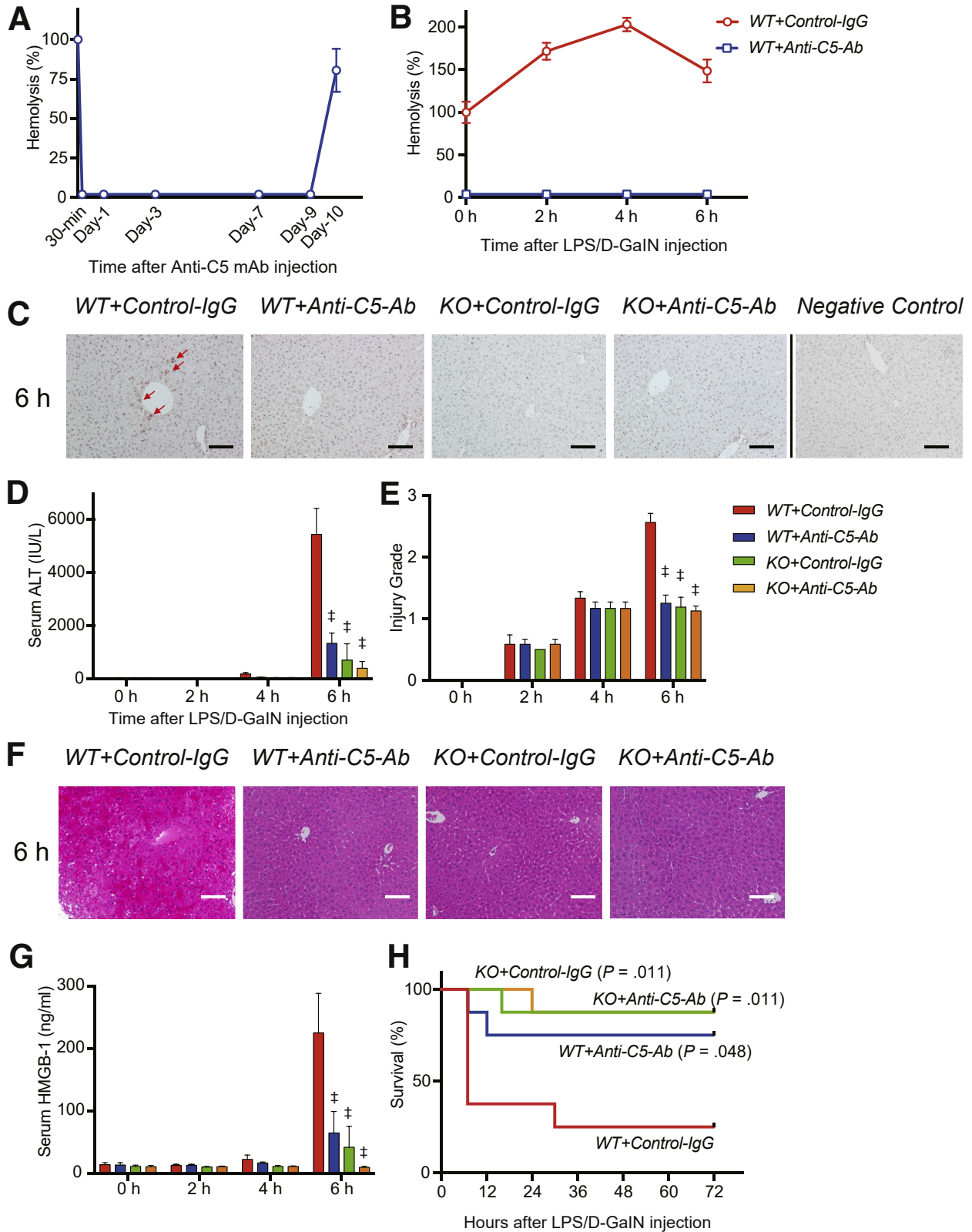
6 hours in *WT+Control-IgG* mice (Figure 1*G*). In contrast, C5-KO and anti-C5-Ab treatment significantly attenuated the HMGB-1 burst at 6 hours.

Animal Survival

To determine whether C5 regulators simply delay liver injury or exert sustained protective effects and prevent mortality, animal survival was assessed after LPS/D-GalN challenge. Among the control mice (*WT+Control-IgG*), 5 of 8 mice died within 8 hours, whereas only 1 died from among *WT+Anti-C5-Ab* mice. No C5-KO mice died within an 8-hour period. Two of 8 (25.0%) wild-type (WT) control mice displayed long-term survival; however, 6 (75.0%) and 7 (87.5%) mice in the anti-C5-Ab and C5-KO groups, respectively, survived for 3 d (Figure 1*H*).

Proinflammatory Cytokines and Chemokines

Proinflammatory cytokines play pivotal roles in ALF pathogenesis. Among macrophage-derived cytokines, tumor necrosis factor α (TNF-α) particularly mediates and exacerbates LPS/D-GalN–induced liver damage.[24,25] CXC chemokines (eg, CXCL-1 and CXCL-2) serve as neutrophil chemoattractants. Both C5-KO and anti-C5-Ab treatment significantly downregulated proinflammatory cytokines and chemokines at the messenger RNA level at 6 hours (Figure 2*A*). TNF-α messenger RNA was significantly downregulated upon C5-KO and anti-C5-Ab treatment at earlier phases of 2 and 4 hours, respectively. Serum TNF-α levels were significantly decreased from 2 hours upon C5-KO and anti-C5-Ab treatment (Figure 2*B*). Thus, liver damage alleviated by C5 regulators was associated with early downregulation of TNF-α but no other proinflammatory cytokine.

C5aR Antagonist and Macrophage Activation

The TNF-α storm early after the LPS/D-GalN challenge was significantly attenuated through C5 inhibition. Because C5aR is expressed on macrophages, and C5a is a potent macrophage chemoattractant,[6,26,27] we investigated whether C5a-C5aR inhibition suppresses proinflammatory macrophage activation. Activated macrophages are one of the major extrahepatic sources of various complement proteins.[28] As shown in Figure 2*C*, C5aR-antagonist significantly and dose-dependently attenuated TNF-α production from activated macrophages, indicating a pivotal role of the anaphylatoxin, C5a, in TNF-α/macrophage-mediated liver damage in ALF.

Platelet Aggregation in Hepatic Microcirculation

Microcirculatory impairment is a pathognomonic feature of ALF.[13,14,29] Platelet thrombi, represented by CD41+ spots, were significantly fewer in *WT+Anti-C5-Ab* and KO mice than in *WT+Control-IgG* at 4 and 6 hours after LPS/D-GalN challenge (Figure 3*A*). Thus, platelet aggregation was significantly suppressed by C5 regulators before the peak of acute liver injury.

Altered Populations of Liver-Resident and Infiltrating Macrophages

C5a is a potent macrophage chemoattractant,[26] and resultant macrophage infiltration indicates ALF exacerbation.[30–32] To examine alterations in macrophage compositions in ALF, we performed immunohistochemical staining for F4/80 and CD11b. F4/80 is a representative marker for macrophages, mainly Kupffer cells, while CD11b is for infiltrating macrophages.[33,34] As shown in Figure 3*B*, the number of F4/80+ cells gradually decreased in the *WT+Control-IgG* mice but was significantly retained in *WT+Anti-C5-Ab* and KO mice.

In contrast, CD11b+ cells were recruited to control livers time dependently. Such macrophage infiltration was significantly attenuated upon C5-KO and anti-C5-Ab treatment from 2 and 4 hours, respectively (Figure 3*B*). Altered macrophage populations (ie, reduced number of Kupffer cells and increased number of infiltrating macrophages) are

---

Figure 1. (*See previous page*). **Hemolytic and complement activity, liver damage, and animal survival.** (*A*) Transition of hemolytic activity in mouse sera after intravenous administration of anti-C5-Ab. Hemolytic activity was completely inhibited immediately after this treatment until day 9 and rapidly recovered on day 10 (n = 3 mice/group at each time point). (*B*) Transition of hemolytic activity in the sera of ALF model mice intravenously administered anti-C5-Ab or control IgG. In *WT+Control-IgG* mice (red line), hemolytic activity peaked 4 hours after LPS/D-GalN injection, approaching 203% of baseline levels. In *WT+Anti-C5-Ab* mice (blue line), hemolytic activity was completely inhibited throughout the study (n = 4 mice/group at each time point). (*C*) Representative liver sections for immunohistochemical staining for C5b-9 at 6 hours after LPS/D-GalN administration (n = 6 mice/group, magnification, ×200). Scale bars = 100 μm. In *WT+Control-IgG* mice, MAC deposition was observed around some central veins (arrows), representing the "mosaic" pattern; however, it was not detected in the other groups. (*D*) In *WT+Control-IgG* mice, serum ALT levels sharply increased at 6 hours. Severe hepatocyte destruction was, however, significantly alleviated upon anti-C5-Ab treatment or C5-KO ($P < .001$). Boxes and bars are mostly invisible until 4 hours, as the values are negligible. All data are presented as mean ± SEM values. Differences among groups were assessed via 2-way repeated-measurement analysis of variance ($P < .001$; n = 8 mice/group), followed by Bonferroni's posttest. ‡$P < .001$ vs *WT+Control-IgG*. (*E*) Histopathological grading (n = 8 mice/group; intergroup difference through the 2-way analysis of variance, $P < .001$; time-point assessment using Bonferroni's posttest, ‡$P < .001$ vs *WT+Control-IgG*). Consistent with ALT release, tissue damage was significantly alleviated upon C5-KO and anti-C5-Ab treatment. (*F*) Representative hematoxylin and eosin–stained liver tissue sections at 6 hours after intravenous LPS/D-GalN administration (magnification, ×200). Scale bar = 100 μm. (*G*) Serum HMGB-1 concentrations after LPS/D-GalN injection sharply increased at 6 hours in *WT+Control-IgG* but were significantly reduced upon C5-KO and anti-C5-Ab treatment (n = 6 mice/group; intergroup difference: $P < .001$; time-point assessment, ‡$P < .001$ vs *WT+Control-IgG*). (*H*) Kaplan-Meier curves plotted after the LPS/D-GalN challenge (n = 8 each). C5-KO and anti-C5-Ab significantly improved overall mortality rates compared with those among *WT+Control-IgG* mice in log-rank tests.
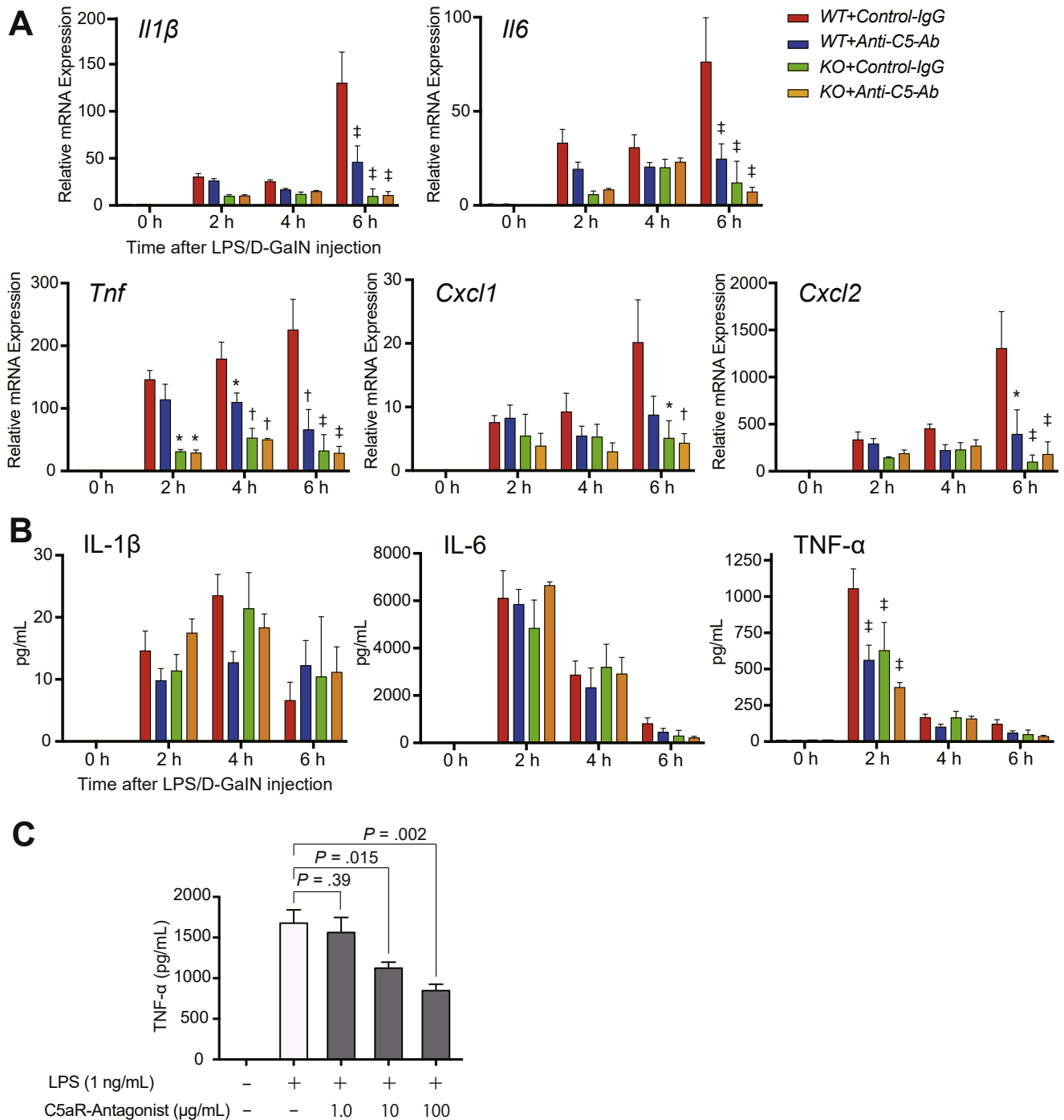
Figure 2. Proinflammatory cytokines and chemokines. (*A*) Quantitative reverse-transcription PCR analysis of expression of proinflammatory cytokines (*Il1β*, *Il6*, and *Tnf*) and chemokines (*Cxcl1* and *Cxcl2*). C5-KO and anti-C5-Ab significantly down-regulated these factors at 6 hours, among which *Tnf* was significantly downregulated earlier from 2 and 4 hours upon C5-KO and anti-C5-Ab treatment, respectively. Data points are not visible owing to negligible values at 0 hours. Gene expression levels were normalized to those of *Gapdh* (mean ± SEM, n = 6 mice/group). The data were represented as fold differences by the $2^{-\Delta\Delta Ct}$ method, with the control mice (*WT+Control-IgG*) at 0 hours as a reference. Differences among the groups were assessed using 2-way analysis of variance ($P < .001$. $P = .001$; $P < .001$, $P = .053$, and $P = .007$ in *Il1β*, *Il6*, *Tnf*, *Cxcl1*, and *Cxcl2*, respectively), followed by Bonferroni's posttest (*$P < .05$; †$P < .01$; ‡$P < .001$ vs *WT+Control-IgG*). (*B*) Serum cytokine concentrations after LPS/D-GalN injection, measured using ELISA. TNF-α levels sharply increased at 2 hours among *WT+Control-IgG* mice and were significantly reduced upon C5-KO and anti-C5-Ab treatment (n = 6 mice/group; intergroup difference: $P = .62$ for IL-1β, $P = .82$ for IL-6, $P = .005$ for TNF-α; time point assessment, ‡$P < .001$ vs *WT+Control-IgG*). (*C*) Peritoneal macrophages were stimulated with LPS in the presence of high C5aR antagonist concentrations (PMX53: 0, 1, 10, and 100 μg/mL). C5aR antagonist significantly and dose-dependently attenuated TNF-α production (mean ± SEM; n = 6 each; Mann-Whitney *U* test).

a pathognomonic feature of acute liver injury.[30–32] These deleterious alterations were significantly attenuated upon C5-KO and anti-C5-Ab treatment.

Neutrophil Infiltration

C5a is a neutrophil chemoattractant,[26] and neutrophils play a pivotal role in inflammatory responses and
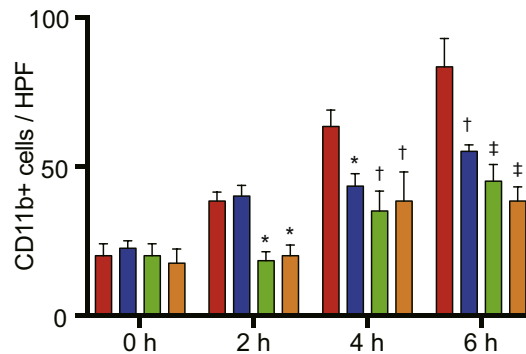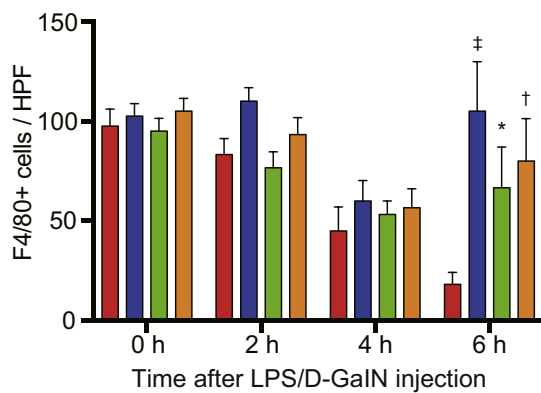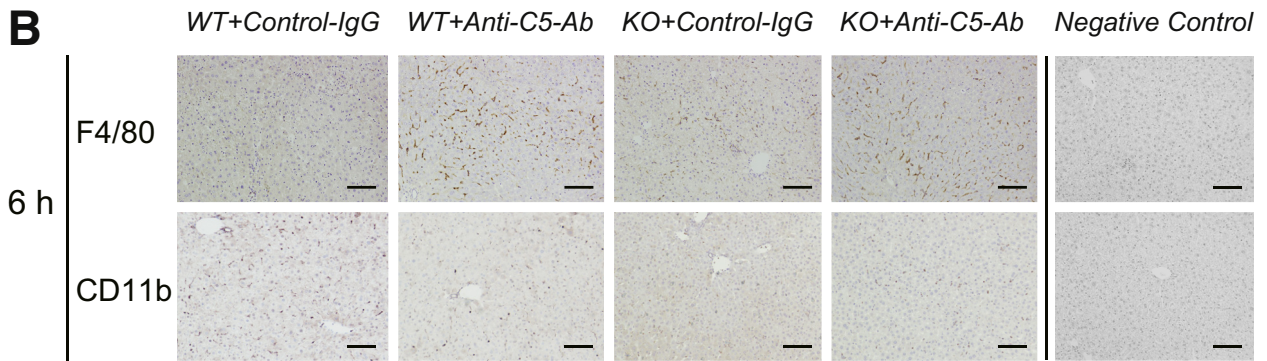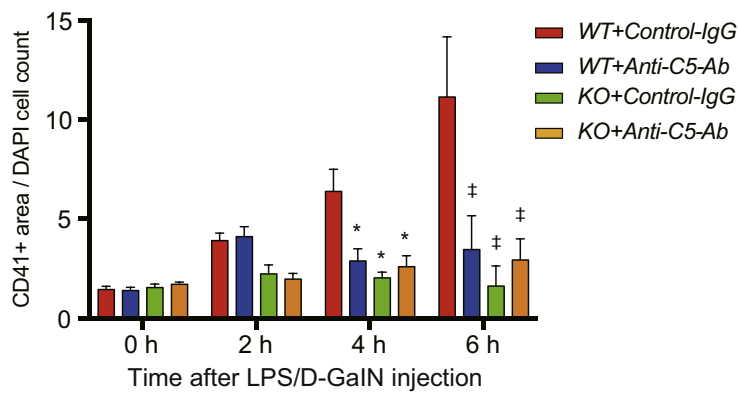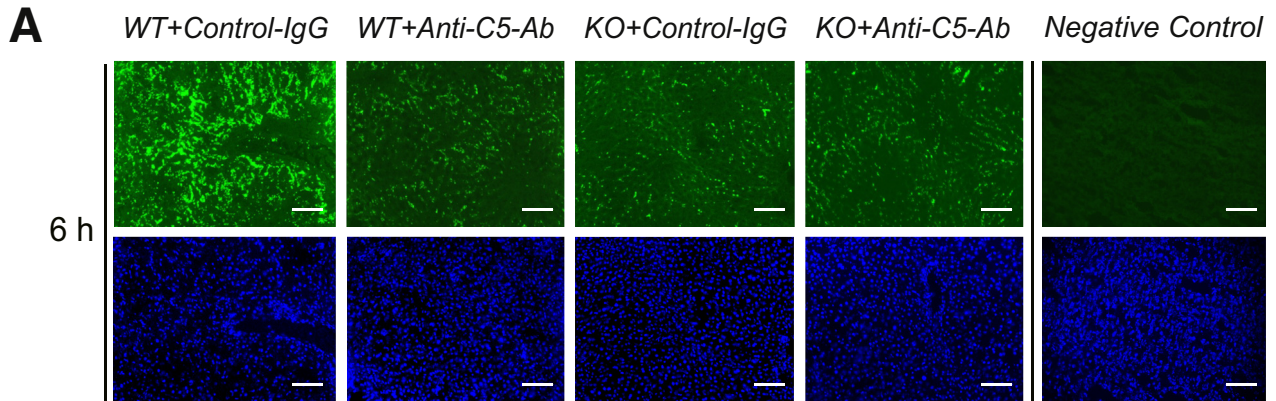
resultant tissue injury in ALF.[25] In this study, the number of Ly6G+ cells (ie, activated neutrophils) sharply increased between 4 and 6 hours after LPS/D-GalN challenge in *WT+Control-IgG* mice (Figure 4A). Furthermore, the number of Ly6-G+ cells was significantly reduced upon C5-KO and anti-C5-Ab treatment after 6 hours, indicating the significant attenuation of neutrophil infiltration through total C5 inhibition.

Oxidative Tissue Damage

The generation of reactive oxygen species and resulting oxidative stress are central pathologies in acute liver injury.[35] The 8-hydroxy-2'-deoxyguanosine (8-OHdG)–positive cells, a sensitive marker for oxidative DNA damage, were diffusely distributed in *WT+Control-IgG* mice; however, they were sporadic around portal venules (zone 1) in the other groups (Figure 4B).

Cell Apoptosis

Because apoptotic hepatocyte death is a major attribute of different liver diseases,[36] we examined apoptosis through single-stranded DNA (ssDNA) staining of liver tissues after LPS/D-GalN exposure. As shown in Figure 4C, the number of ssDNA-positive cells markedly increased between 4 and 6 hours after LPS/D-GalN administration in *WT+Control-IgG* mice, which was significantly attenuated in *WT+Anti-C5-Ab* and KO mice.

c-Jun N-Terminal Kinase Signaling and Caspase Expression

Because C5-KO and anti-C5-Ab suppressed apoptosis by 80% and 70%, respectively, we comprehensively assessed the upstream signaling pathways leading to apoptosis, including c-jun N-terminal kinase (JNK) signaling and caspases.[24,37–41] As shown in Figure 5, only JNK activation was downregulated upon C5-KO and anti-C5-Ab treatment at 2 hours. Furthermore, downstream cascades, caspase-8/-9 activation, cytochrome c (Cyt C) release, and the subsequent cleavage of caspase-3/-7 was assessed at 2 and 4 hours using Western blotting. Cleaved caspase-8 and -9 and Cyt C levels were lower in *WT+Anti-C5-Ab* and KO mice than in *WT+Control-IgG* mice at 4 hours. Consequently, cleaved caspase-3 and -7 levels at 4 hours were also lower in *WT+Anti-C5-Ab* and KO mice than in *WT+Control-IgG* mice.

Total C5 vs Selective C5a Inhibition in LPS/D-GalN–Induced Liver Injury

A selective C5aR antagonist, PMX53, was used to compare the hepatoprotective effects of total C5 and C5a inhibitors. Serum ALT was significantly decreased by treatment with anti-C5-Ab than that with the C5aR antagonist at 6 hours after LPS/D-GalN injection (Figure 6A). Furthermore, anti-C5-Ab treatment reduced pathological grades and HMGB-1 release compared with the C5aR antagonist, demonstrating superior hepatoprotection through total C5 inhibition than selective C5a blockade (Figure 6B and C).

Delayed Doses of Anti-C5-Ab: Effective or Not?

In clinical practice, ALF patients are always encountered after the manifestation of symptoms. Therefore, therapeutic agents must be effective even upon treatment after the onset of liver damage. Therefore, we investigated whether delayed doses of anti-C5-Ab after LPS/D-GalN challenge were effective. Serum ALT, pathological grades, and HMGB-1 release at 6 hours after LPS/D-GalN injection were significantly improved upon anti-C5-Ab treatment at 2 hours, and this effect was comparable to that upon simultaneous administration (Figure 6D–F). Although these differences were not significant for each parameter, even a 4-hour delay in anti-C5-Ab administration reduced liver injury.

Anti-C5-Ab in Concanavalin-A–Induced ALF: Protective or Not?

Concanavalin-A (Con-A)–induced hepatitis is an established ALF model with immune-mediated liver injury depending on T-cells and TNF signaling.[24,38,42] Serum ALT, histological grading, and HMGB-1 release were all significantly ameliorated upon anti-C5-Ab treatment and C5-KO at 4 hours (Figure 6G–I). Regarding animal survival (Figure 6J), all mice died within 24 hours in the *WT+Control-IgG* group; however, 50.0%, 75.0%, and 87.5% of mice survived throughout the study period in the *WT+Anti-C5-Ab* ($P = .007$), *KO+Control-IgG* ($P < .001$), and *KO+Anti-C5-Ab* ($P < .001$) groups, respectively.

Discussion

This study showed the therapeutic effect of C5 inhibition on ALF and the underlying mechanisms. Total C5 inhibition through anti-C5-Ab treatment significantly alleviated LPS/D-GalN–induced liver injury, which was comparable with

Figure 3. (*See previous page*). **Platelet aggregation and altered macrophage populations.** (*A*) Representative tissue sections stained for CD41 at 6 hours after LPS/D-GalN challenge (magnification, ×200; scale bar = 100 μm) and their quantification using ImageJ. CD41+ particles (ie, intrahepatic platelet thrombi) were significantly fewer in *WT+Anti-C5-Ab* and KO mice than in *WT+Control-IgG* at 4 and 6 hours. (*B*) Immunohistochemical staining for F4/80+ and CD11b+ cells at 6 hours (magnification, ×200; scale bar = 100 μm) and their quantification using ImageJ. F4/80+ cells were gradually reduced in *WT+Control-IgG* mice; however, they were significantly retained in *WT+Anti-C5-Ab* and KO mice at 6 hours. In contrast, CD11b+ cells were recruited to control livers in a time-dependent manner, which was significantly attenuated upon C5-KO and anti-C5-Ab treatment from 2 and 4 hours, respectively. All data are presented as mean ± SEM values (n = 6 mice/group). Intergroup differences: $P < .001$, $P = .007$, and $P < .001$ for CD41, F4/80, and CD11b, respectively, and time point assessment by posttests: *$P < .05$, †$P < .01$, ‡$P < .001$ vs *WT+Control-IgG*.

the effect of C5-KO, and surpassed C5a inhibition only. Considering that ALF patients visit the hospital only upon symptom onset, delayed doses of anti-C5-Ab after the onset of liver injury also confer significant hepatoprotection. Moreover, C5 regulators were effective against Con-A–induced ALF, characterized by different etiologies. These
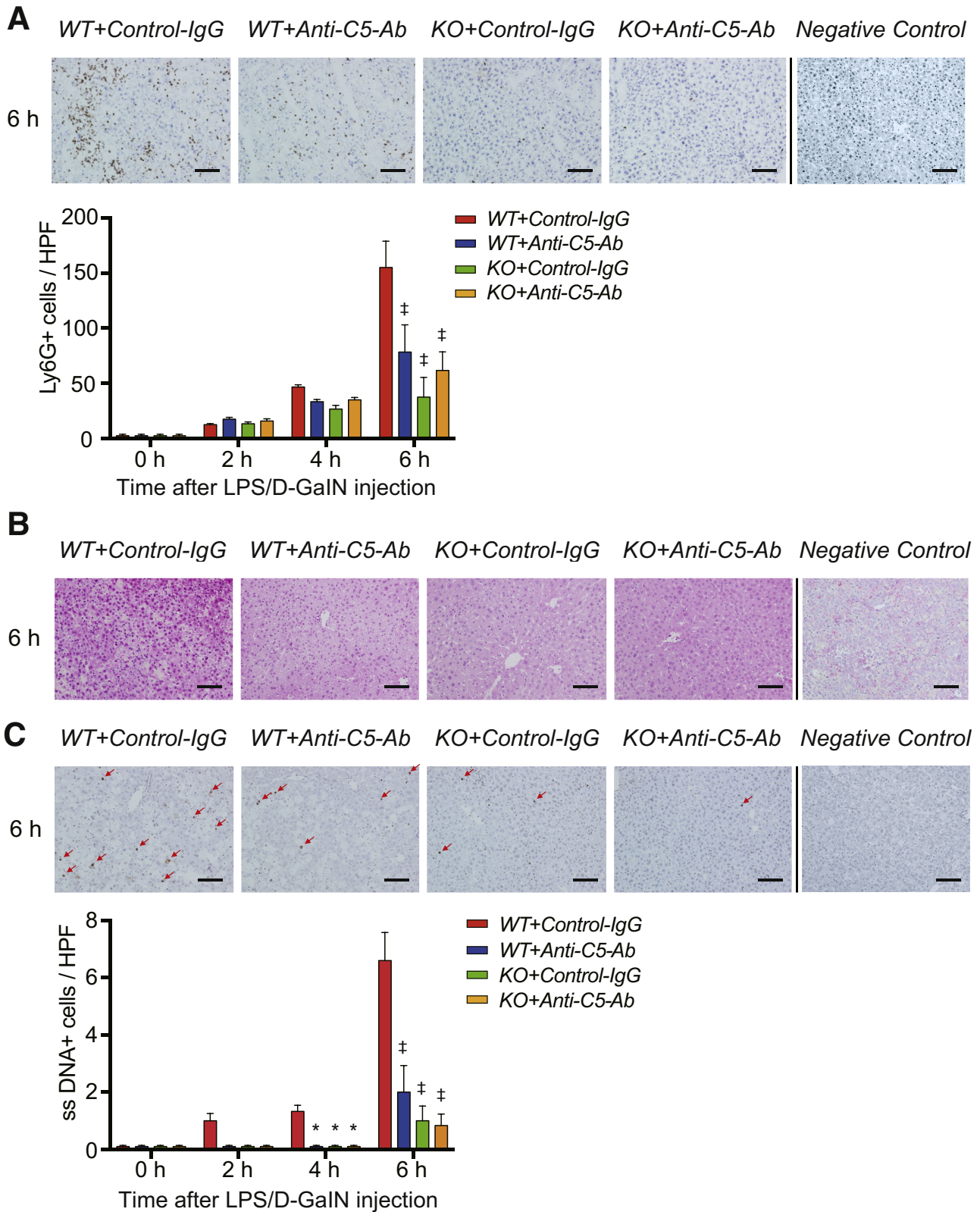
results highlight the therapeutic potential of anti-C5-Ab in deterring progression of acute and fulminant hepatitis to ALF, regardless of the underlying etiologies.

C5a is a well-known anaphylatoxin that enhances leukocyte activation and transmigration and promotes vascular permeability and vasoconstriction.[43] These reactions occur when C5a binds to C5aR, which is expressed on various cells, including macrophages, neutrophils, and platelets.[6,27] In this study, the therapeutic effects of C5 regulators were observed in various cells at different time points. TNF-α production by macrophages was reduced from the early stage of liver injury, accompanied by reduced sinusoidal platelet aggregation. Neutrophil activation was inhibited at the late stage. These phenomena are interlinked and should not be interpreted separately. However, the inhibitory effects on C5a-C5aR interactions, a central player in ALF progression,[12–14] on various effectors significantly attenuate acute liver injury in a cooperative manner.

In contrast to that of C5a, the potential role of MAC in ALF pathogenesis remains unclear. On comparing the efficacy of total C5 and selective C5aR inhibition, we elucidated the significance of MAC, an innate effector that generates cytotoxic pores on microbial cell surfaces, in ALF. Moreover, MAC promotes interleukin (IL)-1β secretion, neutrophil recruitment, and caspase activation through NLRP3 inflammasome activation[20,21,44] and induces the release of α-granules and microparticles from platelets, stimulating their procoagulant activity by augmenting prothrombinase.[44] Hence, MACs may be intricately involved in the upregulation of inflammatory mediators and cause microcirculatory dysfunction, both being crucial to ALF pathogenesis.[13,14,39]

Furthermore, anti-C5-Ab treatment significantly reduced TNF-α production early after LPS/D-GalN administration. Notably, our in vitro study indicated that the C5aR-antagonist decreased TNF-α production from activated macrophages in the absence of other complement-related factors. Aside from hepatocytes, activated macrophages produce complement components including C3a and C5a, thereby eliciting their auto-stimulation.[27,45] C5a regulation by anti-C5-Ab mitigates this bidirectional feedback loop both locally and systemically. Similar to LPS/D-GalN–induced liver injury, Con-A–induced hepatitis is reportedly TNF dependent,[24] as revealed through significant reduction in hepatocyte death in *TNF*-KO animals.[46,47] Consequently, significant TNF-α downregulation in the early phase

through C5 regulation helped markedly alleviate ALF in this study.

Apoptosis in hepatocytes is mediated through the extrinsic, death receptor–dependent pathway and the intrinsic, mitochondrial-dependent pathway.[23,41,48,49] Death ligands include FasL, TNF-α, and TNF-related apoptosis-inducing ligand. The extrinsic pathway is activated through the interaction of death ligands with death receptors. Caspase-8 is initially triggered, followed by activation of the effector caspase cascade including caspase-3 and -7. The intrinsic pathway is characterized by Cyt C release and caspase-9 activation, which further promotes the effector caspase cascade. In this study, C5 regulation significantly attenuated the activation of both the extrinsic and intrinsic pathways in ALF. Inhibition of the latter is critical for alleviating liver injury because it amplifies the effector caspase cascade in TNF-α/TNR receptor-1–mediated hepatocyte apoptosis.[48,50]

JNK, an upstream signal before caspase cleavage, plays a critical role in LPS/D-GalN– and Con-A–induced hepatocyte apoptosis.[37,51] Concurrently, this study showed that JNK phosphorylation was significantly suppressed through C5 inhibition in LPS/D-GalN–induced ALF. C5b-9 directly induces JNK-dependent necrotic cell death[52]; however, it remains unknown whether C5 and its derivatives directly activate JNK-mediated apoptosis in hepatocytes. In this study, it is plausible that C5 inhibitor–mediated reduction in TNF-α levels interfered with JNK activation, leading to caspase-8 cleavage and Cyt C release.[41,53,54] However, the precise role of JNK in TNF-α–mediated hepatocyte damage remains controversial. Das et al[24] reported that JNK is essential for TNF-α expression in hematopoietic cells but not in hepatocytes. Moreover, they reported comparable liver damage through TNF-α in both hepatocyte-specific JNK1/2-KO and control mice. The question remains whether C5 regulation reduces hepatocyte apoptosis directly by inhibiting JNK-mediated downstream caspases or indirectly by downregulating TNF-α.

In addition to the aforementioned unresolved issue, a potential limitation may exist regarding the application of the C5aR antagonist, PMX-53, thus inhibiting the major type of C5aR, CD88, but not the minor type, C5L2.[55] Both receptors are expressed on similar cells, and a functional association between the 2 has been suggested. However, CD88 was markedly upregulated compared with C5L2,[55] and C5L2 may merely function as a decoy receptor. Thus, the

---

Figure 4. (*See previous page*). **Neutrophil infiltration, oxidative stress, and apoptosis.** (*A*) Immunohistochemical staining for Ly6-G at 6 hours after LPS/D-GalN (magnification, ×200; scale bar = 100 μm) and their quantification using ImageJ. The number of Ly6G+ cells was sharply increased at 6 hours in *WT+Control-IgG* mice; however, neutrophil infiltration was significantly suppressed in *WT+Anti-C5-Ab* and KO mice. (*B*) Representative liver sections stained with the oxidative stress marker, 8-OHdG at 6 hours (n = 6 mice/group, magnification, ×200; scale bar =) 100 μm). The staining intensity of 8-OHdG was high in nuclei sustaining severe DNA damage. Positive cells were diffusely distributed in *WT+Control-IgG* mice but sporadic around portal venules (zone-1) in the other groups. (*C*) Representative ssDNA staining of liver sections at 6 hours after LPS/D-GalN challenge (magnification, ×200; scale bar = 100 μm) and its quantification (ImageJ). The number of ssDNA+ cells (arrows) was markedly increased at 6 hours in *WT+Control-IgG* mice, which was significantly attenuated upon C5-KO and anti-C5-Ab treatment. All data are presented as mean ± SEM values (n = 6 mice/group). Intergroup difference: $P < .001$ for Ly6G and ssDNA, and Bonferroni's posttests: *$P < .05$ and ‡$P < .001$ vs *WT+Control-IgG*. HPF, high-power field; Ly6-G, lymphocyte antigen 6 complex locus G.
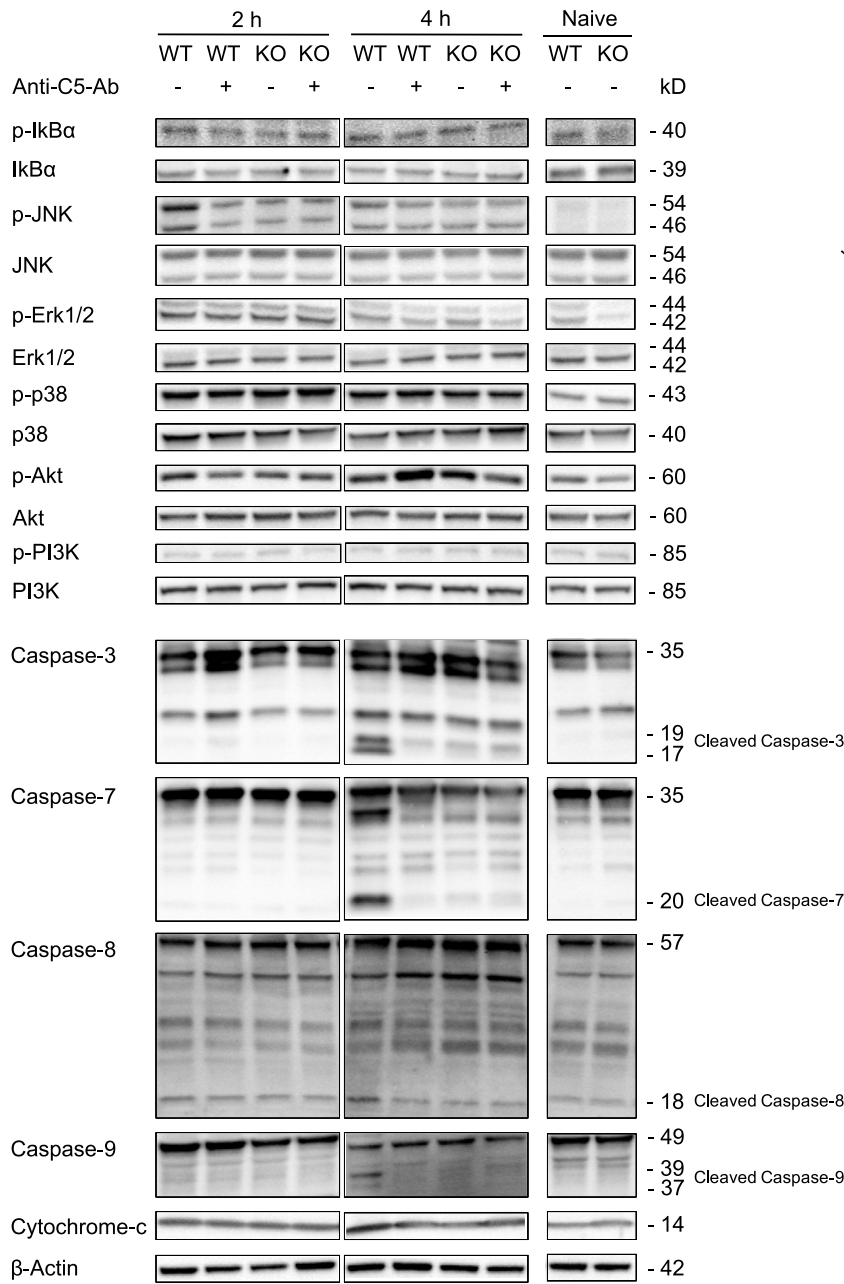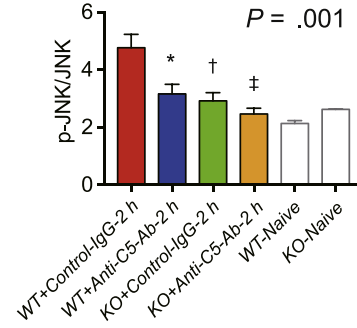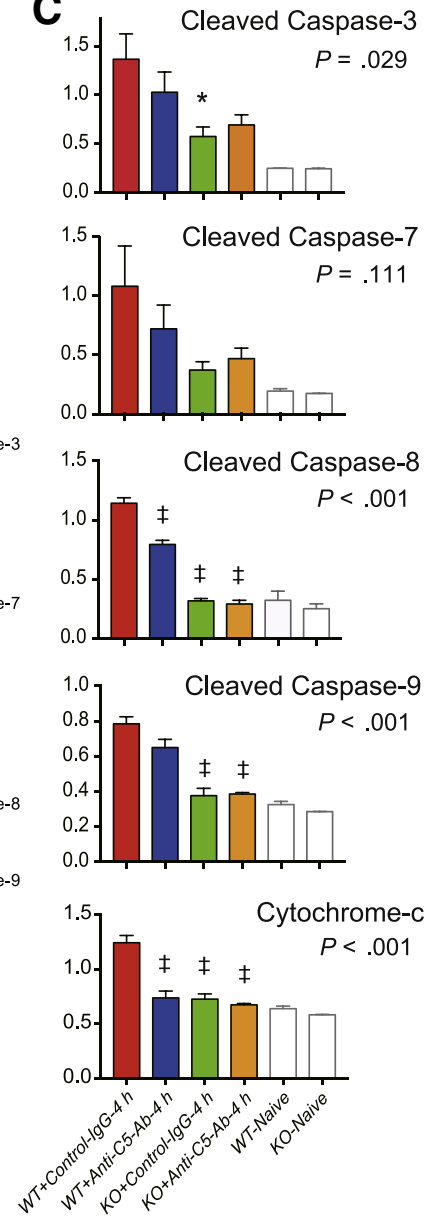
Figure 5. Western blots for caspases and upstream signals. (A) JNK phosphorylation at 2 hours after LPS/D-GalN challenge was significantly suppressed upon C5-KO and anti-C5-Ab treatment, leading to significant downregulation of caspase-3, -7, -8, -9, and Cyt C at 4 hours. Notably, C5-KO and anti-C5-Ab treatment did not affect any other signal. (B, C) Protein expression levels were quantified using ImageJ and normalized to those of (B) JNK and (C) β-actin (mean ± SEM, n = 5 mice/group; *$P < .05$, ‡$P < .001$ vs WT+Control-IgG).

therapeutic antagonism of CD88 has been evaluated only in clinical trials on C5a-C5aR inhibition.[56] Therefore, it is reasonable to focus on CD88 inhibition to evaluate methods for C5a-C5aR blockade.

In conclusion, this study showed that total C5 inhibition by anti-C5-Ab treatment exerts a marked therapeutic effect on 2 different ALF mice models. The efficacy of total C5 inhibition was superior to that of C5a blockade in LPS/D-
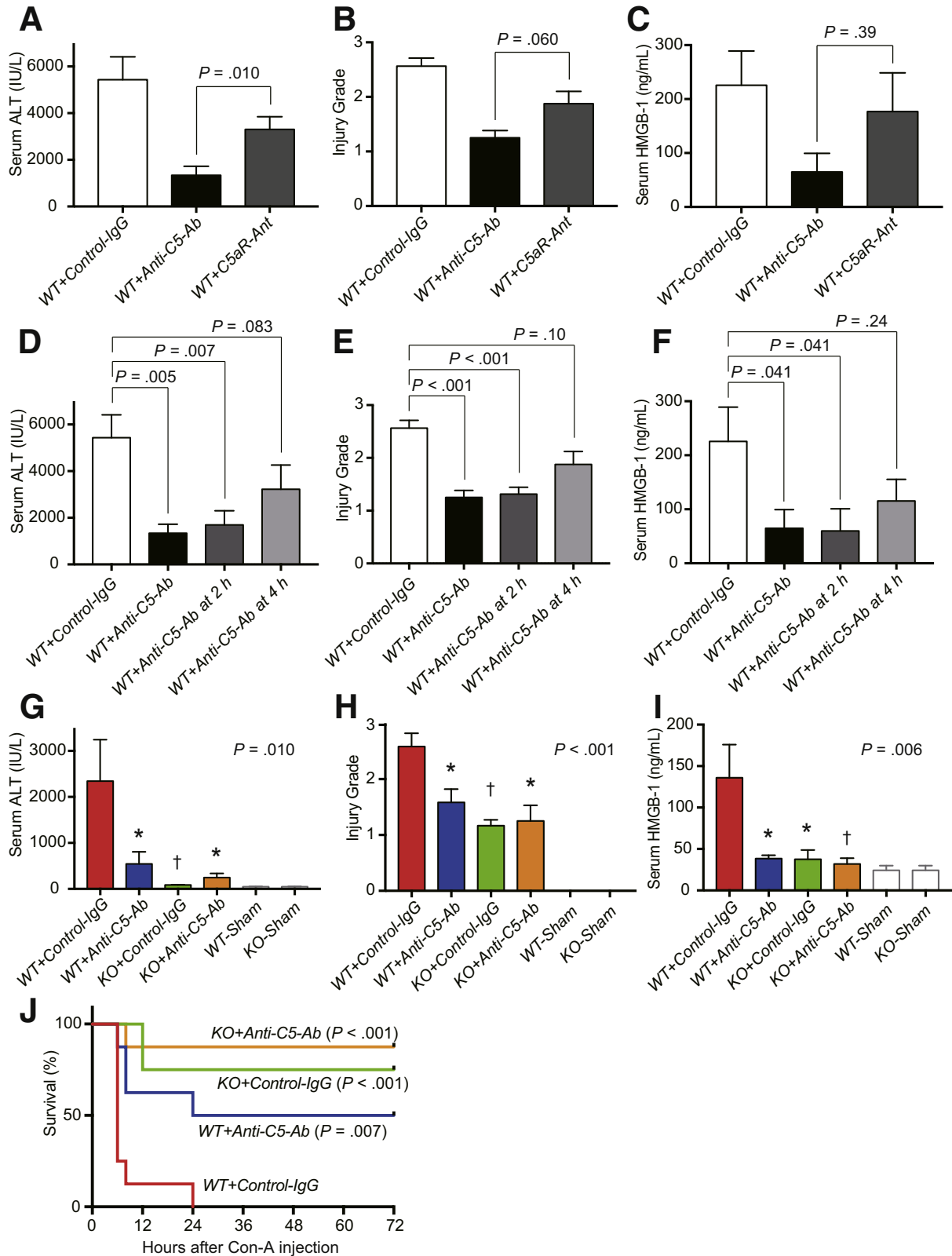
GalN–induced liver injury. Considering its significant hepatoprotective effects even with delayed doses after the onset of liver injury and increased information regarding clinical safety, anti-C5-Ab potentially provides a novel promising strategy to inhibit the progression of acute hepatitis to ALF.

Materials and Methods

Animals

Male WT, B10D2nSn-Slc (C5+/+) and KO, B10D2oSn-J (C5–/–) mice (8–10 weeks old, 20–25 g) were purchased from Japan SLC (Hamamatsu, Japan) and the Jackson Laboratory (Bar Harbor, ME), respectively. All animals were housed under specific pathogen-free conditions in a temperature- and humidity-controlled environment with a 12-hour light/dark cycle and were provided ad libitum access to tap water and standard chow pellets. All animals received humane care in accordance with the ARRIVE (Animal Research: Reporting of In Vivo Experiments) guidelines. All experimental protocols were approved by the Animal Research Committee of Kyoto University (MedKyo-17546 and -18193). All authors had access to the study data and had reviewed and approved the final manuscript.

Murine Models of ALF

Mice were anesthetized with isoflurane and intraperitoneally administered LPS (30 μg/kg, from *Escherichia coli* O111:B4; Sigma-Aldrich, St. Louis, MO)/D-GalN (400 mg/kg; Wako Pure Chemical Corporation, Osaka, Japan) followed by intravenous administration of anti-C5-Ab, BB5.1,[57] provided by Alexion Pharmaceuticals (Cheshire, CT), at 60 mg/kg. Thereafter, they were euthanized, and liver and blood samples were obtained 2, 4, and 6 hours after the LPS/D-GalN injection. Liver tissues were sampled from the left posterior segment, and blood was sampled from the vena cava. Control WT and KO mice were treated with the same dose of control immunoglobulin (mouse IgG1 isotype control, clone MOPC-21; Bio X Cell, Lebanon, NH) instead of anti-C5-Ab. Furthermore, WT mice were treated with C5aR-antagonist (PMX53; Tocris Bioscience, Minneapolis, MO),[58] a cyclic hexapeptide AcF (OpdChaWR), at 1 mg/kg.[13,58,59] Sham-operated mice were intraperitoneally administered sterile phosphate-buffered saline. To assess the efficacy of anti-C5-Ab in another mouse model of ALF induced through a different method, additional mice were intravenously administered 30 mg/kg of Con-A (Wako Pure Chemical Corporation).[24,42]

Complement Hemolytic Assay

Terminal complement activity in mouse sera was assessed using the standard method, including its ability to lyse presensitized chicken erythrocytes with erythrocyte-specific Abs, as previously reported.[11,60] The results were confirmed using another hemolytic assay. Briefly, the extent of hemolysis of unsensitized sheep erythrocytes was determined by incubating them with mouse serum in the presence of zymosan. In this so-called reactive lysis, erythrocytes are lysed if the complement cascade is activated in the serum, rather than on erythrocyte membranes.

Assessment of Hepatocellular Damage

Serum ALT levels in peripheral blood, an indicator of hepatocellular injury, were determined using a standard spectrophotometric method with an automated clinical analyzer (JCA-BM9030; Jeol, Tokyo, Japan).

Histological Analysis

Paraffin-embedded liver tissue specimens were cut into 4-μm-thick sections and stained with hematoxylin and eosin. The severity of liver damage (steatosis, apoptosis/necrosis, or inflammation) was graded by 2 independent pathologists in a blinded manner as follows: 0, absent; 0.5, minimal; 1, mild; 1.5, mild to moderate; 2, moderate; 2.5, moderate to marked; 3, marked.[25,39]

Enzyme-Linked Immunosorbent Assay

Serum HMGB-1 levels were quantified using the HMGB-1 ELISA Kit II (Shino-Test, Tokyo, Japan) in accordance with the manufacturer's protocol. Serum IL-1β, IL-6, and TNF-α levels were measured using Mouse Quantikine ELISA Kits (R&D Systems, Minneapolis, MN) in accordance with the manufacturer's instructions.

Quantitative Reverse-Transcription Polymerase Chain Reaction Analysis

Genes encoding proinflammatory cytokines (*Il1b*, *Il6*, and *Tnf*) and chemokines (*Cxcl1* and *Cxcl2*) in liver tissues treated with or without C5 regulators were subjected to quantitative reverse-transcription polymerase chain reaction (PCR) analysis. Briefly, total RNA was extracted from liver tissues, using an RNeasy Kit (Qiagen, Venlo, the Netherlands) and complementary DNA was prepared using an Omniscript RT kit (Qiagen), as reported previously.[11]

Figure 6. (*See previous page*). **Total C5 vs selective C5a inhibition in LPS/D-GalN–induced ALF.** (*A*) Serum ALT, (*B*) histopathological grades, and (*C*) HMGB-1 release at 6 hours after LPS/D-GalN challenge were ameliorated through anti-C5-Ab treatment, rather than that with the C5aR antagonist. Delayed doses of anti-C5-antibody: effective or not? (*D*) Serum ALT, (*E*) histopathological grades, and (*F*) HMGB-1 release at 6 hours after LPS/D-GalN challenge. Anti-C5-Ab treatment at 2 hours after LPS/D-GalN injection was as effective in reducing liver damage as the simultaneous injection. Although the differences were not significant for each parameter, anti-C5-Ab treatment at 4 hours still lowered liver injury. Differences among groups were assessed using the Mann-Whitney *U* test (vs *WT+Control-IgG*, mean ± SEM, n = 6–8 mice/group). Anti-C5 antibody in Con-A–induced ALF: protective or not? (*G*) Serum ALT, (*H*) histopathological injury grades, and (*I*) HMGB-1 release at 4 hours after Con-A administration. All parameters were significantly improved upon C5-KO and anti-C5-Ab treatment (n = 6-8 mice/group; *P < .05, †P < .01 vs *WT+Control-IgG*). (*J*) Kaplan-Meier curves after Con-A challenge (n = 8 each). C5-KO and anti-C5-Ab treatment significantly improved the overall mortality rates (P < .001 and P = .007 vs *WT+Control-IgG* by log-rank test, respectively).

Thereafter, quantitative reverse-transcription PCR was performed using the StepOnePlus Real-Time PCR System (Life Technologies, Tokyo, Japan). The following primers were used to amplify specific gene fragments: GAPDH forward (f) 5′-TGTGTCCGTCGTGGATCTGA-3′, reverse (r) 5′-TTGCTGTTGAAGTCGCAGGAG-3′; IL-1β (f) 5′-GGTCAAAGGTTTGGAAGCAG-3′, (r) 5′-TGTGAAATGC-CACCTTTTGA-3′; IL-6 (f) 5′-ACCAGAGGAAATTTTCAA-TAGGC-3′, (r) 5′-TGATGCACTTGCAGAAAACA-3′; TNF-α (f) 5′-AGGGTCTGGGCCATAGAACT-3′, (r) 5′-CCACCACGCTCTTCTGTCTAC-3′; CXCL-1 (f) 5′-TCTCCGTTACTTGGGGACAC-3′, (r) 5′-CCACACTCAA-GAATGGTCGC-3′; CXCL-2 (f) 5′-TCCAGGTCAGTTAGCCTTGC-3′, (r) 5′-CGGTCAAAAAGTTTGCCTTG-3′. Target gene expression levels were normalized to those of the house-keeping gene, *Gapdh*. The data were represented as fold differences by the 2$^{-\Delta\Delta Ct}$ method, where $\Delta Ct = Ct_{target\ gene} - Ct_{GAPDH}$ and $\Delta\Delta Ct = \Delta Ct_{induced} - \Delta Ct_{reference}$, with the control mice (*WT+Control-IgG*) at 0 hours as a reference.

Immunohistochemistry

Liver tissue specimens were deparaffinized, antigen retrieval was performed using citrate buffer (10 mM, pH 6.0). After blocking with Protein Block Serum-Free (X0909, DAKO, Tokyo, Japan), sections were incubated with rat mAb against mouse F4/80 (#14-4801, 1:50, eBioscience, San Diego, CA), mouse mAb against 8-OHdG (clone N45.1, 1:10; Japan Institute for the Control of Aging, Nikken SEIL, Shizuoka, Japan), and rabbit polyclonal Abs against mouse C5b-9 (#ab55811, 1:1000; Abcam, Cambridge, United Kingdom), mouse CD11b (#ab75476, 1:400, Abcam), and mouse ssDNA (#18731, 1:600; IBL, Fujioka, Japan). Rat mAbs against mouse CD41 (MWReg30, 1:100; GeneTex, Irvine, CA) and lymphocyte antigen 6 complex locus G (Ly6-G) (#5931, 1:10; Tonbo Biosciences, Irvine, CA) were applied to frozen liver sections. For light microscopy, sections were treated with biotinylated rabbit anti-rat immunoglobulin G (IgG) and goat anti-rabbit IgG (1:300). After incubation, immunoperoxidase (VECTASTAIN Elite ABC Kit; Vector Labs, Burlingame, CA) was applied, and then the sections were visualized using DAB (Sigma-Aldrich) solution with hematoxylin counterstaining. Exceptionally, Avidin-biotin-alkaliphosphatase complex (VECTASTAIN ABC-AP Standard Kit; Vector Labs) and Fast Red (Fast Red II Substrate kit; Nichirei Biosciences, Tokyo, Japan) were used for visualization for 8-OHdG staining instead of avidin-peroxidase complex and DAB because endogenous peroxidase activity was not blocked by H_2O_2, which produces hydroxiradical, converting deoxyguanosine into 8-OHdG. For fluorescence microscopy, sections were treated with Alexa 488-conjugated goat anti-rat IgG (1:500) and covered with Vectashield mounting medium containing DAPI (Vector Labs). The sections were observed using a BZ-9000 fluorescence microscope (Keyence, Osaka, Japan). Positive cells were enumerated in a blinded manner from 10 high-magnification fields per section (×400). Negative controls were generated through incubation with normal rat IgG or rabbit IgG (sc-2026, -2027; Santa Cruz Biotechnology, Santa Cruz, CA) instead of the initial Abs. The CD41-positive area was quantified using ImageJ version 1.51 (National Institutes of Health, Bethesda, MD).

Western Blot Analysis

Liver tissues were homogenized in radio-immunoprecipitation buffer (Thermo Fisher Scientific, Waltham, MA), soluble protein lysates (30 μg/sample) were subjected to sodium dodecyl sulfate polyacrylamide gel electrophoresis (12% resolving gel), and the protein bands were electrotransferred onto polyvinylidene difluoride membranes (Bio-Rad, Hercules, CA). After blocking the membranes with 5% skim milk, they were probed with unconjugated primary antibodies in the dilution buffer (0.5% skim milk in Tris-buffered saline-Tween 20) with overnight agitation at 4°C. Rabbit mAbs against mouse caspase-3 (#14220, 1:1000), caspase-7 (#12827, 1:1000), Cyt C (#11940, 1:1000), p-IkBα (#2859, 1:1000), p-JNK (#4671, 1:1000), p-ERK1/2 (#4370, 1:2000), p-p38 (#4511, 1:1000), p-Akt (#4060, 1:2000), IkBα (#4812, 1:1000), ERK1/2 (#4695, 1:1000), p38 (#8690, 1:1000), Akt (#4691, 1:1000), and PI3K (#4257, 1:1000), and rabbit polyclonal Abs against mouse caspase-9 (#9504, 1:1000), p-PI3K (#4228, 1:1000), and JNK (#9252, 1:1000) were purchased from Cell Signaling Technology (Danvers, MA). Rabbit polyclonal Ab against mouse caspase-8 (#AF1650, 1:400) was purchased from R&D Systems (Minneapolis, MN). Rabbit polyclonal Ab against mouse β-Actin (#PM053, 1:2000) was purchased from MBL (Nagoya, Japan). After being washed, the membranes were probed with horse-radish peroxidase-conjugated secondary antibody (P0448; DAKO, Santa Clara, CA). Chemiluminescence was detected using ImmunoStar Zeta (Wako Pure Chemical Industries, Osaka, Japan), and the protein signals were visualized using a charge-coupled device camera (EZ-capture; Atto Corporation, Tokyo, Japan). Protein band intensity was quantified using ImageJ.

In Vitro Assays for TNF-α from Macrophages

Thirty additional WT mice were intraperitoneally administered 1.5 mL of 4% Brewer thioglycolate medium (Sigma-Aldrich). Four days later, thioglycolate-elicited peritoneal macrophages were harvested through peritoneal lavage with RPMI 1640 medium (Thermo Fisher Scientific). The extracted cells were enumerated and suspended in the same medium supplemented with 10% heat-inactivated fetal bovine serum (Thermo Fisher Scientific), -U/mL penicillin (Thermo Fisher Scientific), 100-μg/mL streptomycin (Thermo Fisher Scientific), 50-μM 2-mercaptoethanol (Thermo Fisher Scientific), and 2-mM L-glutamine (Thermo Fisher Scientific). Macrophages were seeded at 2.0 × 10^5 cells in 0.5 mL/well into 24-well cell-culture plates and incubated in a humidified atmosphere of 5% CO_2 and 95% air. After 3 hours, the wells were washed thrice with phosphate-buffered saline to eliminate nonadherent cells and then incubated with or without LPS (1 ng/mL) and several concentrations of C5aR antagonist

(n = 6 each). Five hours later, the supernatants were harvested and stored at -80°C until ELISA.

Statistical Analysis

All data are expressed as mean ± SEM values. Differences among experimental groups were analyzed using 2-way analysis of variance, followed by post hoc tests at each time point to compare therapeutic effects with those in the control mice (*WT+Control-IgG*), if appropriate. Kaplan-Meier analysis and the log-rank test were performed to assess survival. The Mann-Whitney *U* test was performed to compare the 2 groups in Figures 2*C* and 6*A*–F. A *P* value <.05 was considered to indicate statistical significance. All tests were performed using Prism 7 (GraphPad Software, San Diego, CA).

References

1. Stravitz RT, Lee WM. Acute liver failure. Lancet 2019; 394:869–881.
2. Wu Z, Han M, Chen T, Yan W, Ning Q. Acute liver failure: mechanisms of immune-mediated liver injury. Liver Int 2010;30:782–794.
3. Laskin DL, Sunil VR, Gardner CR, Laskin JD. Macrophages and tissue injury: agents of defense or destruction? Annu Rev Pharmacol Toxicol 2011;51:267–288.
4. Reuben A, Tillman H, Fontana RJ, Davern T, McGuire B, Stravitz RT, Durkalski V, Larson AM, Liou I, Fix O, Schilsky M, McCashland T, Hay JE, Murray N, Shaikh OS, Ganger D, Zaman A, Han SB, Chung RT, Smith A, Brown R, Crippin J, Harrison ME, Koch D, Munoz S, Reddy KR, Rossaro L, Satyanarayana R, Hassanein T, Hanje AJ, Olson J, Subramanian R, Karvellas C, Hameed B, Sherker AH, Robuck P, Lee WM. Outcomes in adults with acute liver failure between 1998 and 2013. Ann Intern Med 2016;164:724.
5. Bernal W, Hyyrylainen A, Gera A, Audimoolam VK, McPhail MJW, Auzinger G, Rela M, Heaton N, O'Grady JG, Wendon J, Williams R. Lessons from look-back in acute liver failure? A single centre experience of 3300 patients. J Hepatol 2013;59:74–80.
6. Barratt-Due A, Thorgersen EB, Pischke SE, Nilsson PH, Haugaa H, Mollnes TE, Harboe M. The role of complement in liver injury, regeneration and transplantation. Hepatology 2019;70:725–736.
7. Rensen SS, Slaats Y, Driessen A, Peutz-Kootstra CJ, Nijhuis J, Steffensen R, Greve JW, Buurman WA. Activation of the complement system in human nonalcoholic fatty liver disease. Hepatology 2009;50:1809–1817.
8. Lee JH, Poudel B, Ki HH, Nepali S, Lee YM, Shin JS, Kim DK. Complement C1q stimulates the progression of hepatocellular tumor through the activation of discoidin domain receptor 1. Sci Rep 2018;8:4908.
9. Hillebrandt S, Wasmuth HE, Weiskirchen R, Hellerbrand C, Keppeler H, Werth A, Schirin-Sokhan R, Wilkens G, Geier A, Lorenzen J, Köhl J, Gressner AM, Matern S, Lammert F. Complement factor 5 is a quantitative trait gene that modifies liver fibrogenesis in mice and humans. Nat Genet 2005;37:835–843.
10. McCullough RL, McMullen MR, Sheehan MM, Poulsen KL, Roychowdhury S, Chiang DJ, Pritchard MT, Caballeria J, Nagy LE. Complement factor d protects mice from ethanol-induced inflammation and liver injury. Am J Physiol Gastrointest Liver Physiol 2018; 315:G66–G79.
11. Kusakabe J, Hata K, Tamaki I, Tajima T, Miyauchi H, Wang Y, Nigmet Y, Okamura Y, Kubota T, Tanaka H, Tsuruyama T, Uemoto S. Complement 5 inhibition ameliorates hepatic ischemia/reperfusion injury in mice, dominantly via the C5a-mediated cascade. Transplantation 2020;104:2065–2077.
12. Sun S, Guo Y, Zhao G, Zhou X, Li J, Hu J, Yu H, Chen Y, Song H, Qiao F, Xu G, Yang F, Wu Y, Tomlinson S, Duan Z, Zhou Y. Complement and the alternative pathway play an important role in LPS/D-GalN–induced fulminant hepatic failure. PLoS One 2011;6:e26838.
13. lian Xu G, Chen J, Yang F, qing Li G, xin Zheng L, zhang Wu Y. C5a/C5aR pathway is essential for the pathogenesis of murine viral fulminant hepatitis by way of potentiating Fgl2/fibroleukin expression. Hepatology 2014;60:114–124.
14. Liu J, Tan Y, Zhang J, Zou L, Deng G, Xu X, Wang F, Ma Z, Zhang J, Zhao T, Liu Y, Li Y, Zhu B, Guo B. C5aR, TNF-α, and FGL2 contribute to coagulation and complement activation in virus-induced fulminant hepatitis. J Hepatol 2014;62:354–362.
15. Hillmen P, Young NS, Schubert J, Brodsky RA, Socié G, Muus P, Röth A, Szer J, Elebute MO, Nakamura R, Browne P, Risitano AM, Hill A, Schrezenmeier H, Fu C, Maciejewski J, Rollins SA, Mojcik CF, Rother RP, Luzzatto L. The complement inhibitor eculizumab in paroxysmal nocturnal hemoglobinuria. N Engl J Med 2006;355:1233–1243.
16. Legendre CM, Licht C, Muus P, Greenbaum LA, Babu S, Bedrosian C, Bingham C, Cohen DJ, Delmas Y, Douglas K, Eitner F, Feldkamp T, Fouque D, Furman RR, Gaber O, Herthelius M, Hourmant M, Karpman D, Lebranchu Y, Mariat C, Menne J, Moulin B, Nürnberger J, Ogawa M, Remuzzi G, Richard T, Sberro-Soussan R, Severino B, Sheerin NS, Trivelli A, Zimmerhackl LB, Goodship T, Loirat C. Terminal complement inhibitor eculizumab in atypical hemolytic–uremic syndrome. N Engl J Med 2013;368:2169–2181.
17. Howard JF, Utsugisawa K, Benatar M, Murai H, Barohn RJ, Illa I, Jacob S, Vissing J, Burns TM, Kissel JT, Muppidi S, Nowak RJ, O'Brien F, Wang JJ, Mantegazza R, Mazia CG, Wilken M, Ortea C, Saba J, Rugiero M, Bettini M, Vidal G, Garcia AD, Lamont P, Leong WK, Boterhoven H, Fyfe B, Roberts L, Jasinarachchi M, Willlems N, Wanschitz J, Löscher W, De Bleecker J, Van den Abeele G, de Koning K, De Mey K, Mercelis R, Wagemaekers L, Mahieu D, Van Damme P, Smetcoren C, Stevens O, Verjans S, D'Hondt A, Tilkin P, Alves de Siqueira Carvalho A, Hasan R, Dias Brockhausen I, Feder D, Ambrosio D, Melo AP, Rocha R, Rosa B, Veiga T, Augusto da Silva L, Gonçalves Geraldo J, da Penha Morita Ananias M, Nogueira Coelho E, Paiva G, Pozo M, Prando N, Dada Martineli Torres D, Fernanda Butinhao C, Coelho E, Renata Cubas Volpe L, Duran G, Gomes da Silva TC,

Otavio Maia Gonçalves L, Pazetto LE, Souza Duca L, Suriane Fialho TA, Gheller Friedrich MA, Guerreiro A, Mohr H, Pereira Martins M, da Cruz Pacheco D, Macagnan AP, de Cassia Santos A, Bulle Oliveira AS, Amaral de Andrade AC, Annes M, Cavalcante Lino V, Pinto W, Miranda C, Carrara F, Souza I, Genge A, Massie R, Campbell N, Bril V, Katzberg H, Soltani M, Ng E, Siddiqi Z, Phan C, Blackmore D, Vohanka S, Bednarik J, Chmelikova M, Cierny M, Toncrova S, Junkerova J, Kurkova B, Reguliova K, Zapletalova O, Pitha J, Novakova I, Tyblova M, Wolfova M, Jurajdova I, Andersen H, Harbo T, Vinge L, Mogensen A, Højgaard J, Witting N, Autzen AM, Pedersen J, Färkkilä M, Atula S, Nyrhinen A, Erälinna JP, Laaksonen M, Oksaranta O, Eriksson J, Harrison T, Desnuelle C, Sacconi S, Soriani MH, Decressac S, Moutarde J, Lahaut P, Solé G, Le Masson G, Wielanek-Bachelet AC, Gaboreau M, Moreau C, Wilson A, Vial C, Bouhour F, Gervais-Bernard H, Merle H, Hourquin C, Lacour A, Outteryck O, Vermersch P, Zephir H, Millois E, Deneve M, Deruelle F, Schoser B, Wenninger S, Stangel M, Alvermann S, Gingele S, Skripuletz T, Suehs KW, Trebst C, Fricke K, Papagiannopoulos S, Bostantzopoulou S, Vlaikidis N, Zampaki M, Papadopoulou N, Mitsikostas DD, Kasioti E, Mitropoulou E, Charalambous D, Rozsa C, Horvath M, Lovas G, Matolcsi J, Szabo G, Szabadosne B, Vecsei L, Dezsi L, Varga E, Konyane M, Gross B, Azrilin O, Greenbereg N, Bali Kuperman H, Antonini G, Garibaldi M, Morino S, Troili F, Di Pasquale A, Filla A, Costabile T, Marano E, Sacca F, Marsil A, Puorro G, Maestri Tassoni M, De Rosa A, Bonanno S, Antozzi C, Maggi L, Campanella A, Angelini C, Cudia P, Pegoraro V, Pinzan E, Bevilacqua F, Orrico D, Bonifati DM, Evoli A, Alboini PE, D'Amato V, Iorio R, Inghilleri M, Fionda L, Frasca V, Giacomelli E, Gori M, Lopergolo D, Onesti E, Gabriele M, Patti F, Salvatore Caramma A, Messina S, Reggio E, Caserta C, Uzawa A, Kanai T, Mori M, Kaneko Y, Kanzaki A, Kobayashi E, Masaki K, Matsuse D, Matsushita T, Uehara T, Shimpo M, Jingu M, Kikutake K, Nakamura Y, Sano Y, Nagane Y, Kamegamori I, Fujii Y, Futono K, Tsuda T, Saito Y, Suzuki H, Morikawa M, Samukawa M, Kamakura S, Shiraishi H, Mitazaki T, Motomura M, Mukaino A, Yoshimura S, Asada S, Kobashikawa T, Koga M, Maeda Y, Takada K, Takada MT, Yamashita Y, Yoshida S, Suzuki Y, Akiyama T, Narikawa K, Tsukita K, Meguro F, Fukuda Y, Sato M, Matsuo H, Fukudome T, Gondo Y, Maeda Y, Nagaishi A, Nakane S, Okubo Y, Okumura M, Funaka S, Kawamura T, Makamori M, Takahashi M, Hasuike T, Higuchi E, Kobayashi H, Osakada K, Taichi N, Tsuda E, Hayashi T, Hisahara S, Imai T, Kawamata J, Murahara T, Saitoh M, Shimohama S, Suzuki S, Yamamoto D, Konno S, Imamura T, Inoue M, Murata M, Nakazora H, Nakayama R, Ikeda Y, Ogawa M, Shirane M, Kanda T, Kawai M, Koga M, Ogasawara J, Omoto M, Sano Y, Arima H, Fukui S, Shimose S, Shinozaki H, Watanabe M, Yoshikawa C, van der Kooi A, de Visser M, Gibson T, Maessen J, de Baets M, Faber C, Keijzers MJ, Miesen M, Kostera-Pruszczyk A, Kaminska A, Kim BJ, Lee CN, Koo YS, Seok HY, Kang HN, Ra HJ, Kim BJ, Cho E Bin,

Lee HL, Min JH, Seok J, Koh DY, Kwon JY, Lee JE, Park SA, Hong YH, Lim JS, Kim MR, Kim SM, hee Kim Y, Lee HS, Shin HY, Hwang EB, Shin MJ, Sazonov D, Yarmoschuk A, Babenko L, Malkova N, Melnikova A, Korobko D, Kosykh E, Pokhabov D, Nesterova Y, Abramov V, Balyazin V, Casasnovas Pons C, Alberti Aguilo M, Homedes-Pedret C, Palacios NJ, Lazaro A, Diez Tejedor E, Fernandez-Fournier M, Lopez Ruiz P, Rodriguez de Rivera FJ, Salvado Figueras M, Gamez J, Salvado M, Cortes Vicente E, Diaz-Manera J, Querol Gutierrez L, Rojas Garcia R, Vidal N, Arribas-Ibar E, Piehl F, Hietala A, Bjarbo L, Lindberg C, Jons D, Andersson B, Sengun I, Ozcelik P, Tuga C, Ugur M, Boz C, Altiparmak D, Gazioglu S, Ozen Aydin C, Erdem-Ozdamar S, Bekircan-Kurt CE, Yilmaz E, Acar NP, Caliskan Y, Efendi H, Aydinlik S, Cavus H, Semiz C, Tun O, Terzi M, Dogan B, Onar MK, Sen S, Cavdar TK, Norwood F, Dimitriou A, Gollogly J, Mahdi-Rogers M, Seddigh A, Maier G, Sohail F, Sathasivam S, Arndt H, Davies D, Watling D, Rivner M, Hartmann JE, Quarles B, Smalley N, Amato A, Cochrane T, Salajegheh M, Roe K, Amato K, Toska S, Wolfe G, Silvestri N, Patrick K, Zakalik K, Katz J, Miller R, Engel M, Bravver E, Brooks B, Plevka S, Burdette M, Sanjak M, Kramer M, Nemeth J, Schommer C, Juel V, Guptill J, Hobson-Webb L, Beck K, Carnes D, Loor J, Anderson A, Lange D, Agopian E, Goldstein J, Manning E, Kaplan L, Holzberg S, Kassebaum N, Pascuzzi R, Bodkin C, Kincaid J, Snook R, Guinrich S, Micheels A, Chaudhry V, Corse A, Mosmiller B, Ho D, Srinivasan J, Vytopil M, Ventura N, Scala S, Carter C, Donahue C, Herbert C, Weiner E, McKinnon J, Haar L, McKinnon N, Alcon K, Daniels K, Sattar N, Jeffery D, McKenna K, Guidon A, David W, Dheel C, Levine-Weinberg M, Nigro C, Simpson E, Appel SH, Lai E, Lay L, Pleitez M, Halton S, Faigle C, Thompson L, Sivak M, Shin S, Bratton J, Jacobs D, Brown G, Bandukwala I, Brown M, Kane J, Blount I, Freimer M, Hoyle JC, Agriesti J, Khoury J, Marburger T, Kaur H, Dimitrova D, Mellion M, Sachs G, Crabtree B, Keo R, Perez EK, Taber S, Gilchrist J, Andoin A, Darnell T, Goyal N, Sakamuri S, So YT, Welsh LW, Bhavaraju-Sanka R, Tobon Gonzalez A, Jones F, Saklad A, Nations S, Trivedi J, Hopkins S, Kazamel M, Alsharabati M, Lu L, Mumfrey-Thomas S, Woodall A, Richman D, Butters J, Lindsay M, Mozaffar T, Cash T, Goyal N, Roy G, Mathew V, Maqsood F, Minton B, Jones HJ, Rosenfeld J, Garcia R, Garcia S, Echevarria L, Pulley M, Aranke S, Berger AR, Shah J, Shabbir Y, Smith L, Varghese M, Gutmann L, Gutmann L, Swenson A, Olalde H, Hafer-Macko C, Kwan J, Zilliox L, Callison K, DiSanzo B, Naunton K, Bilsker M, Sharma K, Reyes E, Cooley A, Michon SC, Steele J, Karam CK, Chopra M, Bird S, Kaufman J, Gallatti N, Vu T, Katzin L, McClain T, Harvey B, Hart A, Huynh K, Beydoun S, Chilingaryan A, Droker B, Lin F, Shah A, Tran A, Akhter S, Malekniazi A, Tandan R, Hehir M, Waheed W, Lucy S, Weiss M, Distad J, Downing S, Strom S, Lisak R, Bernitsas E, Khan O, Kumar Sriwastava S, Tselis A, Jia K, Bertorini T, Arnold T, Henderson K, Pillai R, Liu Y, Wheeler L, Hewlett J, Vanderhook M, Dicapua D, Keung B, Kumar A, Patwa H, Robeson K, Nye J, Vu H.

Safety and efficacy of eculizumab in anti-acetylcholine receptor antibody-positive refractory generalised myasthenia gravis (REGAIN): a phase 3, randomised, double-blind, placebo-controlled, multicentre study. Lancet Neurol 2017;16:976–986.

18. Misawa S, Kuwabara S, Sato Y, Yamaguchi N, Nagashima K, Katayama K, Sekiguchi Y, Iwai Y. Safety and efficacy of eculizumab in Guillain-Barré syndrome: a multicentre , double-blind, randomised phase 2 trial. Lancet Neurol 2018;4422:1–11.

19. Pittock SJ, Berthele A, Fujihara K, Kim HJ, Levy M, Palace J, Nakashima I, Terzi M, Totolyan N, Viswanathan S, Wang K-C, Pace A, Fujita KP, Armstrong R, Wingerchuk DM. Eculizumab in aquaporin-4–positive neuromyelitis optica spectrum disorder. N Engl J Med 2019;381:614–625.

20. Triantafilou K, Hughes TR, Triantafilou M, Morgan BP. The complement membrane attack complex triggers intracellular Ca2+ fluxes leading to NLRP3 inflammasome activation. J Cell Sci 2013;126:2903–2913.

21. Inoue Y, Shirasuna K, Kimura H, Usui F, Kawashima A, Karasawa T, Tago K, Dezaki K, Nishimura S, Sagara J, Noda T, Iwakura Y, Tsutsui H, Taniguchi S, Yanagisawa K, Yada T, Yasuda Y, Takahashi M. NLRP3 regulates neutrophil functions and contributes to hepatic ischemia-reperfusion injury independently of inflammasomes. J Immunol 2014;192:4342–4351.

22. Wang W, Sun L, Deng Y, Tang J. Synergistic effects of antibodies against high-mobility group box 1 and tumor necrosis factor-α antibodies on <scp>d</scp>-(+)-galactosamine hydrochloride/lipopolysaccharide-induced acute liver failure. FEBS J 2013;280:1409–1419.

23. Luedde T, Kaplowitz N, Schwabe RF. Cell death and cell death responses in liver disease: mechanisms and clinical relevance. Gastroenterology 2014; 147:765–783.e4.

24. Das M, Sabio G, Jiang F, Rincón M, Flavell RA, Davis RJ. Induction of hepatitis by JNK-mediated expression of TNF-α. Cell 2009;136:249–260.

25. Ilyas G, Zhao E, Liu K, Lin Y, Tesfa L, Tanaka KE, Czaja MJ. Macrophage autophagy limits acute toxic liver injury in mice through down regulation of interleukin-1β. J Hepatol 2016;64:118–127.

26. Monk PN, Scola A-M, Madala P, Fairlie DP. Function, structure and therapeutic potential of complement C5a receptors. Br J Pharmacol 2007;152:429–448.

27. Morgan BP, Gasque P. Extrahepatic complement biosynthesis: where, when and why? Clin Exp Immunol 1997;107:1–7.

28. Lubbers R, van Essen MF, van Kooten C, Trouw LA. Production of complement components by cells of the immune system. Clin Exp Immunol 2017;188:183–194.

29. Groeneveld D, Cline-Fedewa H, Baker KS, Williams KJ, Roth RA, Mittermeier K, Lisman T, Palumbo JS, Luyendyk JP. Von Willebrand factor delays liver repair after acetaminophen-induced acute liver injury in mice. J Hepatol 2020;72:146–155.

30. Holt MP, Cheng L, Ju C. Identification and characterization of infiltrating macrophages in acetaminophen-induced liver injury. J Leukoc Biol 2008;84:1410–1421.

31. Zigmond E, Samia-Grinberg S, Pasmanik-Chor M, Brazowski E, Shibolet O, Halpern Z, Varol C. Infiltrating monocyte-derived macrophages and resident kupffer cells display different ontogeny and functions in acute liver injury. J Immunol 2014;193:344–353.

32. Tacke F. Review Targeting hepatic macrophages to treat liver diseases. J Hepatol 2017;66:1300–1312.

33. Yue S, Zhou H, Wang X, Busuttil RW, Kupiec-Weglinski JW, Zhai Y. Prolonged ischemia triggers necrotic depletion of tissue-resident macrophages to facilitate inflammatory immune activation in liver ischemia reperfusion injury. J Immunol 2017; 198:3588–3595.

34. Kageyama S, Nakamura K, Fujii T, Ke B, Sosa RA, Reed EF, Datta N, Zarrinpar A, Busuttil RW, Kupiec-Weglinski JW. Recombinant relaxin protects liver transplants from ischemia damage via hepatocyte glucocorticoid receptor: from bench-to-bedside. Hepatology 2018;68:258–273.

35. Schwabe RF, Brenner DA. Mechanisms of liver injury. I. TNF-α-induced liver injury: Role of IKK, JNK, and ROS pathways. Am J Physiol Gastrointest Liver Physiol 2006; 290:583–589.

36. Brenner C, Galluzzi L, Kepp O, Kroemer G. Decoding cell death signals in liver inflammation. J Hepatol 2013; 59:583–594.

37. Wang Y, Singh R, Lefkowitch JH, Rigoli RM, Czaja MJ. Tumor necrosis factor-induced toxic liver injury results from JNK2-dependent activation of caspase-8 and the mitochondrial death pathway. J Biol Chem 2006; 281:15258–15267.

38. An J, Harms C, Lättig-Tünnemann G, Sellge G, Mandić AD, Malato Y, Heuser A, Endres M, Trautwein C, Donath S. TAT-apoptosis repressor with caspase recruitment domain protein transduction rescues mice from fulminant liver failure. Hepatology 2012; 56:715–726.

39. Zhao E, Ilyas G, Cingolani F, Choi JH, Ravenelle F, Tanaka KE, Czaja MJ. Pentamidine blocks hepatotoxic injury in mice. Hepatology 2017;66:922–935.

40. Deng Y, Ren X, Yang L, Lin Y, Wu X. A JNK-dependent pathway is required for TNFα-induced apoptosis. Cell 2003;115:61–70.

41. Dhanasekaran DN, Reddy EP. JNK signaling in apoptosis. Oncogene 2008;27:6245–6251.

42. Zuo D, Yu X, Guo C, Wang H, Qian J, Yi H, Lu X, Lv ZP, Subjeck JR, Zhou H, Sanyal AJ, Chen Z, Wang XY. Scavenger receptor a restrains T-cell activation and protects against concanavalin A-induced hepatic injury. Hepatology 2013;57:228–238.

43. Ward Peter A, Sarma VJ. New developments in C5a receptor signaling. Cell Heal Cytoskelet 2012;4:73–82.

44. Wiedmer T, Sims PJ. Participation of protein kinases in complement C5b-9-induced shedding of platelet plasma membrane vesicles. Blood 1991;78:2880–2886.

45. Kolev M, Friec G Le, Kemper C. Complement-tapping into new sites and effector systems. Nat Rev Immunol 2014;14:811–820.

46. Küsters S, Tiegs G, Alexopoulou L, Pasparakis M, Douni E, Künstle G, Bluethmann H, Wendel A,

Pfizenmaier K, Kollias G, Grell M. In vivo evidence for a functional role of both tumor necrosis factor (TNF) receptors and transmembrane TNF in experimental hepatitis. Eur J Immunol 1997;27:2870–2875.

47. Maeda S, Chang L, Li ZW, Luo JL, Leffert H, Karin M. IKKβ is required for prevention of apoptosis mediated by cell-bound but not by circulating TNFα. Immunity 2003; 19:725–737.

48. Cao L, Quan XB, Zeng WJ, Yang XO, Wang MJ. Mechanism of hepatocyte apoptosis. J Cell Death 2016;9:19–29.

49. Schwabe RF, Luedde T. Apoptosis and necroptosis in the liver: a matter of life and death. Nat Rev Gastroenterol Hepatol 2018;15:738–752.

50. Imao M, Nagaki M, Imose M, Moriwaki H. Differential caspase-9-dependent signaling pathway between tumor necrosis factor receptor- and Fas-mediated hepatocyte apoptosis in mice. Liver Int 2006;26:137–146.

51. Data S, Cruz S. Induction of hepatitis by JNK-mediated expression of TNF-α. Cell 2009;136:249–260.

52. Gancz D, Donin N, Fishelson Z. Involvement of the c-jun N-terminal kinases JNK1 and JNK2 in complement-mediated cell death. Mol Immunol 2009;47:310–317.

53. Kamata H, Honda SI, Maeda S, Chang L, Hirata H, Karin M. Reactive oxygen species promote TNFα-induced death and sustained JNK activation by inhibiting MAP kinase phosphatases. Cell 2005;120:649–661.

54. Chang L, Kamata H, Solinas G, Luo JL, Maeda S, Venuprasad K, Liu YC, Karin M. The E3 ubiquitin ligase itch couples JNK activation to TNFα-induced cell death by inducing c-FLIPL turnover. Cell 2006;124:601–613.

55. Woodruff TM, Nandakumar KS, Tedesco F. Inhibiting the C5–C5a receptor axis. Mol Immunol 2011;48:1631–1642.

56. Ricklin D, Mastellos DC, Reis ES, Lambris JD. The renaissance of complement therapeutics. Nat Rev Nephrol 2017;14:26–47.

57. Wang Y, Rollins SA, Madri JA, Matis LA. Anti-C5 monoclonal antibody therapy prevents collagen-induced arthritis and ameliorates established disease. Proc Natl Acad Sci U S A 1995;92:8955–8959.

58. Morgan M, Bulmer AC, Woodruff TM, Proctor LM, Williams HM, Stocks SZ, Pollitt S, Taylor SM, Shiels IA. Pharmacokinetics of a C5a receptor antagonist in the rat after different sites of enteral administration. Eur J Pharm Sci 2008;33:390–398.

59. Strey CW, Markiewski M, Mastellos D, Tudoran R, Spruce LA, Greenbaum LE, Lambris JD. The proinflammatory mediators C3a and C5a are essential for liver regeneration. J Exp Med 2003;198:913–923.

60. Wang H, Arp J, Liu W, Faas SJ, Jiang J, Gies DR, Ramcharran S, Garcia B, Zhong R, Rother RP. Inhibition of terminal complement components in presensitized transplant recipients prevents antibody-mediated rejection leading to long-term graft survival and accommodation. J Immunol 2007;179:4451–4463.

Correspondence
Address correspondence to: Koichiro Hata, MD, PhD, Department of Surgery, Division of Hepato-Biliary-Pancreatic Surgery and Transplantation, Kyoto University Graduate School of Medicine, Organ Transplant Unit, Kyoto University Hospital, Kawahara-cho 54, Shogoin, Sakyo-ku, Kyoto city, Kyoto 606-8397, Japan. e-mail: khata@kuhp.kyoto-u.ac.jp; fax: +81-75-751-4348.